C Journal of Carbon Research

MDPI

Article

High Performance of Alkaline Anion-Exchange Membranes Based on Chitosan/Poly (vinyl) Alcohol Doped with Graphene Oxide for the Electrooxidation of Primary Alcohols

Leticia García-Cruz [1], Clara Casado-Coterillo [2], Ángel Irabien [2], Vicente Montiel [1,3] and Jesus Iniesta [1,3,*]

1 Institute of Electrochemistry, University of Alicante, Alicante 03080, Spain; leticia.garcia@ua.es (L.G.-C.); vicente.montiel@ua.es (V.M.)
2 Department of Chemical and Biomolecular Engineering, University of Cantabria, Santander 39005, Spain; clara.casado@unican.es (C.C.-C.); irabienj@unican.es (Á.I.)
3 Department of Physical Chemistry, University of Alicante, Alicante 03080, Spain
* Correspondence: jesus.iniesta@ua.es; Tel.: +34-96-5909850

Academic Editor: Vijay Kumar Thakur
Received: 20 February 2016; Accepted: 24 March 2016; Published: 1 April 2016

Abstract: Mixed matrix membranes (MMM) based on chitosan (CS) and poly (vinyl) alcohol (PVA) with a 50:50 w/w ratio doped with graphene oxide (GO) are prepared by solution casting and characterized by scanning electron microscopy (SEM), X-ray diffraction (XRD), thermogravimetric analysis (TGA), water uptake, alcohol permeability, ion exchange capacity (IEC) and OH^- conductivity measurements. The SEM analysis revealed a dense MMM where the GO nanosheets were well dispersed over the entire polymer matrix. The incorporation of GO increased considerably the thermal stability of the CS:PVA membrane. The GO-based MMM exhibited a low conductivity of 0.19 mS$\cdot$ cm^{-1} in part because the GO sheets did not change the crystallinity of the CS:PVA matrix. The reinforced structure created by the hydrogen bonds between the GO filler and the CS:PVA matrix resulted to be a good physical barrier for alcohol permeability, achieving a coefficient of diffusion of 3.38×10^{-7} and 2.43×10^{-7} cm$^2\cdot$ s^{-1} after 60 and 120 min, respectively, thus avoiding additional alcohol crossover. Finally, the electrochemical performance of the GO-based MMM in the electrooxidation of propargyl alcohol was investigated in a Polymer Electrolyte Membrane Electrochemical Reactor (PEMER) under alkaline conditions, through the polarization curve and the electrolysis reactions, showing a performance comparable to anion-exchange commercial membranes.

Keywords: graphene oxide; graphene composite electrolyte membrane; chitosan; poly (vinyl) alcohol; alkaline anion-exchange membrane (AAEM); alcohol permeability

1. Introduction

The development of membrane technology and its versatility in terms of structure and properties has led to the existence of a large number of membranes in multiple applications. Nowadays, membranes are a key component in energy conversion and storage [1], and more recently, in the less well-known field of organic electrosynthesis [2–5]. In this regard, Polymer Electrolyte Membrane Electrochemical Reactor (PEMER) configuration based on ion-exchange Polymer Electrolyte Membrane (PEM) and Direct Alcohol Fuel Cells (DAFCs) has been employed for the electrooxidation of an unsaturated alcohol to its corresponding carboxylic acids in alkaline medium [6]. The use of alkaline media offers several advantages in terms of the minimization of corrosive reactions compared when using acidic media, the possibility of not needing perfluorated ion-exchange membranes or

precious metals as catalysts, crossover reduction, and a fast electrode kinetic for oxygen reduction reaction (ORR). Moreover, some electroorganic syntheses are more favorable at high pH value [7,8].

The membrane used in PEM electrochemical architectures in alkaline media acts as electrolyte by transferring the hydroxide anions from the cathode to the anode, and provides a barrier separator to the fuel or reactant. Therefore, a high OH^- conductivity and a low alcohol permeability, as well as adequate chemical, mechanical and thermal stability are essential membrane requirements in order to achieve a high performance of the electrochemical process. However, commercial anion-exchange membranes for fuel cell applications still exhibit several limitations in terms of thermal, physical and mechanical properties and low chemical stability [9–11].

Membrane manufacture and performance are attracting great attention in academia and industry in a wide variety of industrial applications. The development of new membranes requires the knowledge of material science and physical chemistry. On the other hand, the chemistry of materials has advanced for the last years, allowing the development of highly featured carbon nanostructures with properties that offer unexpected opportunities in many fields such as adsorption for removal of water-soluble aromatic compounds, CO_2 adsorption, biomedical and electrochemical applications [12,13]. Hence, it is being demonstrated that the introduction of carbon chemistry in polymer materials offers multiple possibilities and improvements in the different electrochemical applications which derivate from the flexible coordination chemistry of carbon atoms and their unique ability to be inserted within the structural framework. To mention some examples, graphene (G) and its derivative forms, such as graphene oxide (GO), sulfonated graphene oxide (sGO) or reduced graphene oxide (rGO), as well as its allotropes, carbon nanotubes [14], are highly promising materials for a wide number of electrochemical processes. The high aspect ratio provides the unique sp^2 nanosheet configuration leading to high surface area and outstanding electrochemical and physical properties such as excellent mechanical and thermal stability, low density, electrical conductivity, and barrier properties. Numerous reports detailed the beneficial implementation of G, GO or sGO in specific electrochemical technologies such as manufacture of enhanced electroanalytical sensors and (bio)sensors [15–17], a multitude of high performance energy conversion and storage devices [18,19], and the preparation of improved nanocomposite materials [20–24], e.g., polymers, among others. GO contains oxygenated groups currently consisting of epoxide, hydroxyl, carbonyl and carboxyl functional groups, which facilitate the binding with the functional groups of the polymer backbone. Therefore, looking for suitable anion-exchange membranes as solid polymer electrolyte (SPE) has led to connect both carbon material and polymer membranes sciences, allowing the development of highly featured carbon nanostructured materials-based polymeric membranes. Several studies have incorporated GO and sGO sheets into polymer membranes providing enhancement of mechanical properties and electrical conductivity, as well as alcohol permeability reduction, with potential applications in a PEM fuel cell configuration [25–33], where chemically modified G are readily dispersed in water or aqueous solutions. Hence, water-soluble polymers are appropriate matrices by their content of hydroxyl groups that facilitates the dispersion and compatibility of modified G fillers in the polymer matrices. A vast number of studies have reported the incorporation of GO, rGO and sGO into biocompatible, eco-friendly and cheap polymers for instance, chitosan (CS) or poly (vinyl) alcohol (PVA) in order to synthetize enhanced nanocomposite materials for a wide number of applications [34–38]. Among them, G-based composite membranes have been used in biological applications such as biosensors for determination of dopamine and uric acid [9], antibacterial material and others biomaterials that require largely improved tensile properties [17,35,39,40], water desalination [41], and pervaporation [42]. Moreover, Ye *et al.* [43] explored the incorporation of GO nanosheets within a PVA matrix to be used as alkaline electrolyte in direct methanol fuel cell, and the same authors described how ionic conductivity, alcohol permeability, and tensile strength depend on the concentration and therefore GO dispersion within the polymer. Movil *et al.* [44] also reported anion-exchange membranes with improved hydroxide conductivity,

and advantageous thermal and mechanical stability from incorporation of functionalized GO into a PVA/poly(diallyldimethylammonium) chloride polymer blend.

Hence, GO is an effective alternative filler to natural clays [21] to achieve reinforced polymers matrix with enhanced structural and physicochemical properties without covalent modification that could affect the striking characteristics of pristine polymeric materials. Recently, carbon nanotubes are incorporated similarly in different polymer structures to enhance their mechanical properties and increase ion conductivities [45–47]. GO nanosheets have increased the glass transition (T_g) and electrochemical properties of chitosan biopolymer (CS) [22].

PVA mixed with CS is often cited in literature for the amelioration of the mechanical, chemical and electrochemical properties of CS in ion-exchange membranes [48,49]. In this respect, the recent work performed by Feng and coworkers described the physicochemical properties of PVA-based membrane incorporating CS polymer and a small amount of rGO or GO fillers [50]. In such work, the advantage of mixing both polymers to a novel reinforced nanocomposite was demonstrated. CS did not only reinforce the PVA matrix by means of strong hydrogen bonds, but it also acted as a bridge between the graphene oxide nanosheets (rGO or GO) and the PVA polymer matrix in aqueous solution, leading to better dispersion of the carbon fillers. The same authors noted that the rGO/CS:PVA and GO/CS:PVA systems showed enhanced conductivity values (loss of crystallinity), thermal and mechanical stability, as well as an increment of T_g from 58.6 to 60.9 °C, and of tensile strength from 35.7 to 48.6 MPa for pure PVA and 0.8 wt.% GO loaded/CS:PVA membranes, respectively. However, to the best of our knowledge, only Yang *et al.* developed a novel anion-exchange membrane based on CS and PVA in 1 to 9 (*w*/*w*) ratio incorporating sG and G for the manufacture of alkaline solid electrolyte membrane for direct alcohol fuel cells applications [51]. These authors achieved a maximum tensile strength of 62.2 $N \cdot mm^{-2}$ using a 0.1 *w*/*w* loading of sG added, with a decrement of crystallinity and increasing conductivities, whose values range between 24 and 47 $mS \cdot cm^{-1}$ with sG and G content, *versus* very slight improvements in terms of thermal stability and alcohol permeability. Besides, their membranes did not exhibit a good dispersion over the entire polymer matrix, probably due mainly to low amount of CS blended with PVA polymer. Finally, GO-based membranes have been recently reviewed for their gas and liquid barrier properties [52] and CS:PVA blend membranes have showed significant increase in mechanical properties of the polymer upon the addition of even low loadings of exfoliated GO nanosheets [20].

Herein, we detail a facile and eco-friendly synthesis of CS and PVA blend polymer membranes based on in a 50:50 *w*/*w* ratio, doped with GO as filler (GO/CS:PVA). An extensive physicochemical characterization of this new GO/CS:PVA membrane was carried out by optical microscopy, scanning electron microscopy (SEM), X-ray diffraction (XRD), water uptake (W_U), X-ray photoelectron spectroscopy (XPS), thermogravimetric analysis (TGA), ion exchange capacity (IEC), alcohol permeability and electrochemical impedance spectroscopy (EIS). Moreover, the Raman analyses were carried out in order to understand how the blend polymer matrix is modified by the incorporation of GO nanosheets. Finally, the performance of GO/CS:PVA membrane was explored through the electrooxidation of a model primary alcohol like propargyl alcohol (PGA) in alkaline medium using a PEM electrochemical reactor configuration.

2. Results and Discussion

2.1. Physicochemical Characterization of Graphene Oxide

TEM micrographs of GO nanosheets are shown in Figure 1A,B. GO nanosheets are clearly identified with a small thickness. According to TEM images, almost fully exfoliated O-functionalized graphene nanosheets are observed. Similar TEM images for GO were observed in [22].

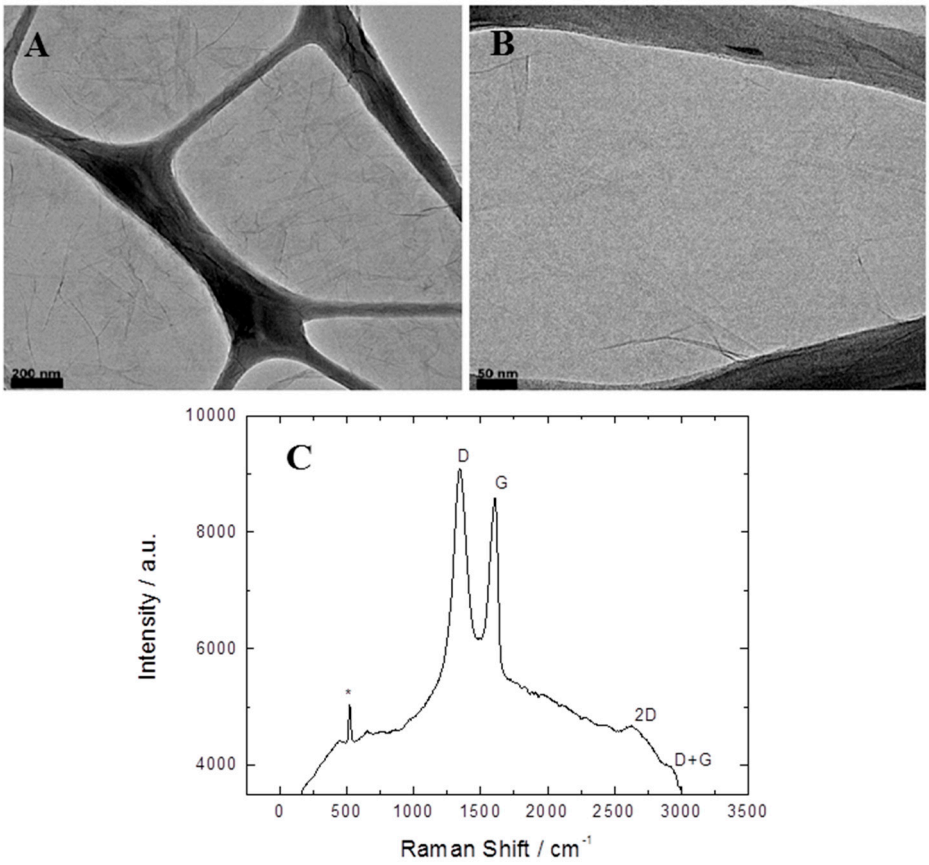

Figure 1. TEM micrographs (**A**,**B**); and Raman spectrum (**C**) of GO. * denotes the Raman spectrum of the SiO_2 wafer.

2.2. Structural and Chemical Characterization of GO/CS:PVA Membrane

Figure 2A,B display the general images of the GO/CS:PVA membrane prepared with 1 wt.% GO with respect to the total weight of polymer mixture. Images are captured after drying process and just before immersing the membrane in alkaline solution to get the OH^- form membrane. The photographs in Figure 2A,B reveal a brownish, homogenous, and smooth surface. Agglomerations corresponding to the incorporation of GO sheets are present in the membrane but homogeneously dispersed, as shown in Figure 2C.

SEM images of the GO/CS:PVA membrane in OH^- form are shown in Figure 3A,B, both surface section and cross section, respectively. The small loading of 1 wt.% GO provides a homogenous surface where the GO sheets are not distinguishable from the polymer matrix, which denotes that the dispersion step through magnetic stirring of GO in CS:PVA mixture of ratio 50:50 (*w*/*w*) was sufficient upon membrane preparation. The homogeneous distribution of GO inside the GO/CS:PVA membrane and the absence of cracks are also demonstrated by the cross section. The incorporation of GO leads to no change on the morphology compared to that obtained from the CS:PVA pristine membrane reported in our previous work [6]. It is worth noting that there are a few little crashes observed in cross section of the membrane, which are mainly attributed to experimental observation under the electron-beam [6].

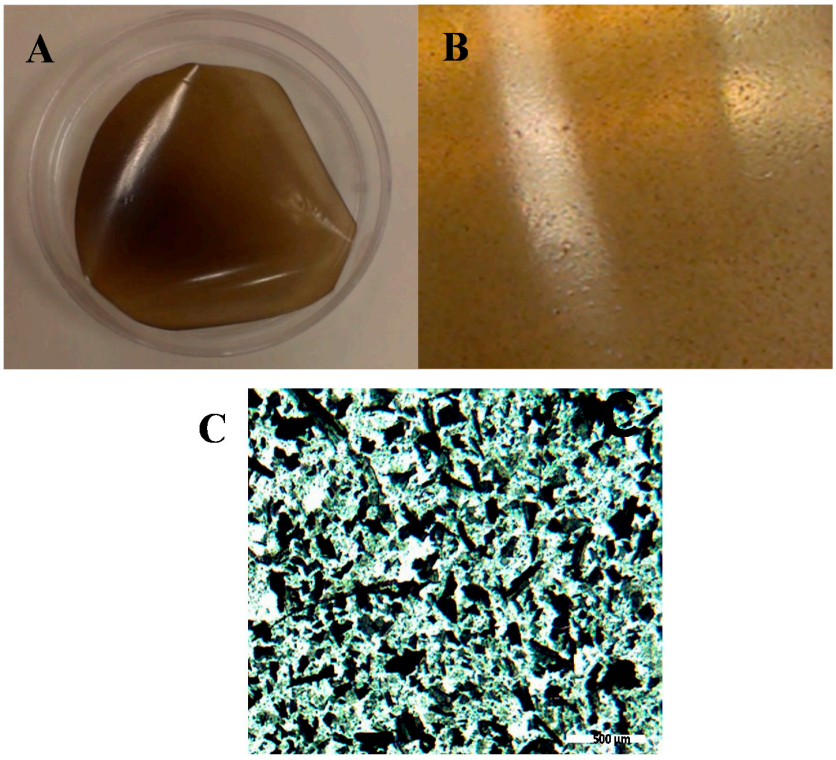

Figure 2. Photographs of the GO/CS:PVA membrane prepared in this work: (**A**) a general view; (**B**) zoom image of the Figure 2A; and (**C**) optical microscopy image.

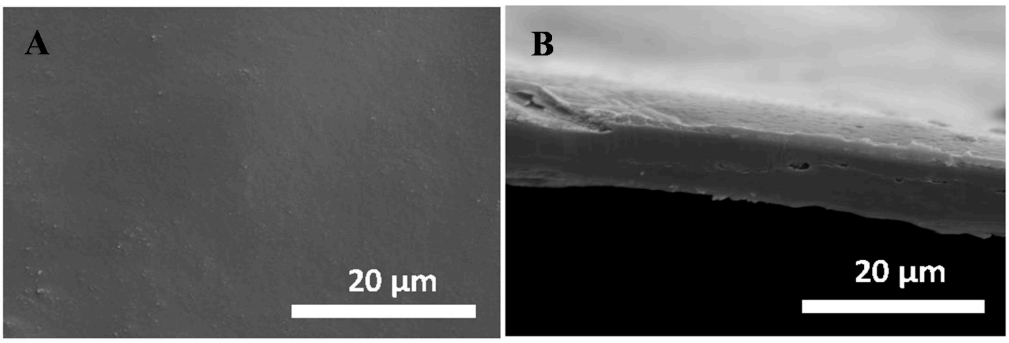

Figure 3. SEM micrographs of the GO/CS:PVA membrane: (**A**) topographical surface; and (**B**) cross-section of the membrane.

Raman spectroscopy is a sensitive technique to symmetric covalent bonds, which allows discerning minor changes in the structural morphology of material, being therefore especially useful for the characterization of the disordered/ordered structure of materials with carbon content. Conjugated and double carbon–carbon bonds provide upper Raman intensities, and the graphitization degree and crystallite size can be calculated from I_D/I_G ratio [20,53]. Figure 4 represents the Raman spectrum of the GO/CS:PVA membrane. This consists of two main bands and two small ones related to the second order region. Typical D and G bands, together with 2D—also known as G' band—and D + G band, are observed for the GO/CS:PVA membrane at 1332, 1598, 2640 and 2925 cm^{-1}, respectively, being the I_D/I_G ratio 1.21, approximately. The position of the G band and the position and shape of 2D band indicate that the GO sheets are present as multilayers in the polymer matrix. In general, a displacement to higher Raman shifts of the 2D band occurs as the layer thickness increases, although the more significant changes are attributed to the band shape, where 2D and D + G bands are much better resolved compared to the second order region shown in Figure 1C, which exhibits a much

broader second order peak near 2650 cm^{-1}. Moreover, D band reveals that GO incorporation gives rise to a material with numerous defects and disorder in part because of O-functionalized groups in GO nanosheets. By comparing the crystalline size of 31.80 nm and 34.35 nm for GO in GO/CS:PVA membrane and GO solution, respectively, it is demonstrated that there is no difference when GO is incorporated within the polymer membrane [20,53].

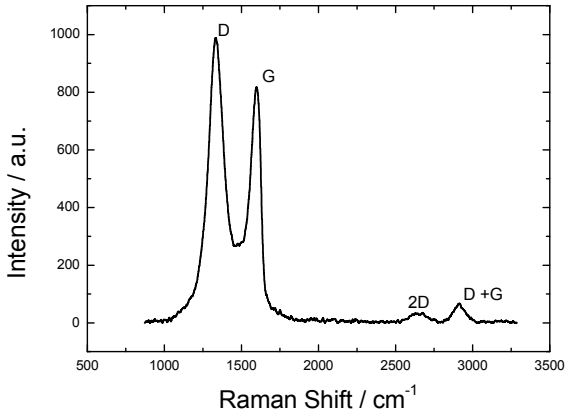

Figure 4. Raman spectrum of GO/CS:PVA membrane.

PVA and CS polymers chain interaction has influence on physical properties such as crystallinity, polymer solubility in, thermal and chemical stability, and ion exchange capacity. The crystallinity can be correlated with the mechanical properties. Figure 5 depicts the X-ray diffractograms of CS:PVA-based membranes where the peaks observed at 10° and 20° can be attributed to both crystal forms of CS polymer [54]. The characteristic diffraction band of PVA appears at 19.5° as described elsewhere [50]. The semi-crystalline character of the CS:PVA blend decreased after the incorporation of the GO filler, although the characteristic diffractogram bands ascribed to the pristine polymers are still observed for the GO/CS:PVA membrane. By comparing with the CS:PVA membrane, slightly broader bands are observed for the GO/CS:PVA membrane than the CS:PVA one. From this, we can conclude that the incorporation of GO in the polymer matrix produces somehow a very slight loss of the crystallinity, as reported for other layered filler additives (AM-4 and UZAR-S3 [55], clay nanotubes [21] or layered double hydroxides [9]). Thus, the GO/CS:PVA membrane is still partially crystalline with both amorphous and crystalline regions influencing positively on the electrical and mechanical properties of the membrane. Our XRD results agree with those obtained by Feng *et al.* [50] and Yang *et al.* [51], who indicated that the incorporation of G and its derivative sheets reduced the crystallinity of CS:PVA membranes, increasing the relative Full Width at Half Maximum (FWHM) value with increasing carbon filler content. However, it must be taken into account that both the CS to PVA polymers ratio and carbon filler were different, as well as the preparation method, including temperature and crosslinking agents that could influence on crystallinity degree [56,57].

XPS analysis of the GO-unfilled and filled CS:PVA membrane together with the GO filler itself are shown in Table 1. Accordingly, the assignment of the binding energy of C, N and O elements reveal no significant difference. Carbonyl and hydroxyl groups are typical functionalization groups with dipoles that interact with dipoles groups present in pristine polymers. The peak for C at 287.9 eV reveals GO layers in the membrane structure attributed to –CO. Furthermore, we have practically found the same values of binding energies of GO in the membrane and GO itself. Consequently, no covalent modification of the GO nanosheets with the polymeric blend was observed that could modify the physicochemical characteristics of the pristine materials. On the other hand, the atomic % of oxygen is also as expected larger for the GO/CS:PVA membrane than for the unfilled polymeric blended membrane as a consequence of the high functionalization degree of the GO filler. The peak related to amino groups coming from CS polymer is present in the spectrum of the GO/CS:PVA membrane at

399.54 and 401.09 eV, which indicates that there is no complexation of N atom with the oxygenated G sheets as filler. In addition, XPS data reveal the presence of carbonyl groups in the CS:PVA-based membrane, denoting the presence of the acetyl groups from the CS polymer (CS is not completely deacetylated, as described in the Experimental Section).

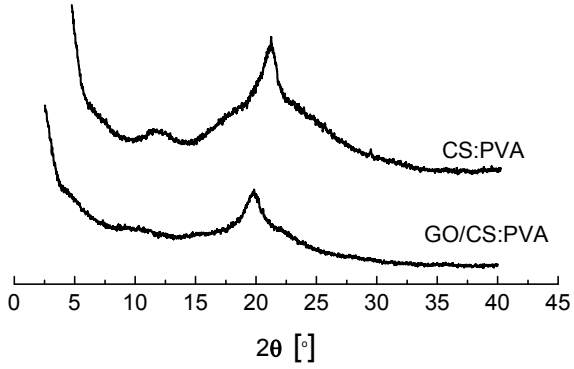

Figure 5. X-ray diffractograms of the CS:PVA and GO/CS:PVA membranes.

Table 1. Deconvolution of the XPS spectra and the assignments based on the binding energy obtained for GO solution, and CS:PVA and GO/CS:PVA membranes.

Element	CS:PVA Membrane	GO Membrane	GO
C 1s	284.29 (40.71) C–C–C–H	284.57 (27.03) Graphite, C–C, C–H	284.56 (32.19) Graphite, C–C, C–H
C 1s	285.85 (25.41) C–N, C–O	286.20 (28.87) C–N, C–O	286.56 (27.18) –C–O
C 1s	287.62 (7.12) –C=O	287.9 (9.47) –C=O	287.81 (9.29) –C=O
C	73.24	65.37	68.66
N 1s	399.15 (4.01) NH–C, NH_2	399.54 (4.69) N–C	
N 1s	400.8 (0.68) C–N	401.09 (0.68) C–N	
N	4.69	5.37	
O 1s	531.03 (5.44) O=C	531.15 (4.14) O=C	531.12 (5.79) O=C
O 1s	532.22 (16.61) O–C	532.49 (25.12) O–C	532.52 (25.55) O–C
O	22.06	29.26	31.34

Thermal stability is a significant requirement of the anion-exchange membrane since they can be utilized under conditions of temperatures up to 100 °C for long time intervals in order to favor the electrochemical processes. In our previous work, the incorporation of PVA in a CS structure provided an increment of about 15 °C in the membrane decomposition temperature with according to TGA analysis under nitrogen atmosphere [6]. Moreover, authors demonstrated that the use of different organic (AS4 and 4VP anionic ionomers) and layered inorganic fillers (stanno and titanosilicates,

UZAR-S3 and AM-4, respectively) led to a slight improvement of the thermal stability of CS:PVA blended membrane. TGA of GO/CS:PVA membrane is displayed in Figure 6 and plots disclose that the incorporation of GO into CS:PVA matrix enhances quite the thermal property of this type of mixed membrane. Figure 6 also displays the three characteristic steps corresponding to: (i) the evaporation of the free water and bound water in the membrane taking place at around 200 °C; (ii) the elimination of side groups of CS and PVA at the temperature ranges of 180–450 °C and 225–480 °C, respectively; and (iii) the breakdown of the polymer from 450 °C for CS and 480 °C for PVA pristine polymers [6]. By contrast, for the GO/CS:PVA membrane, the major weight loss takes place at a temperature range between 250 and 520 °C, after the evaporation of water that can be both bound to the polymer chain and in the interlayer distances between GO sheets (the interlayer distance is increased with O-functionalization groups). By comparing the TGA analysis of CS:PVA and GO/CS:PVA membranes, the later exhibits a major thermal stability reflected in a considerably lower loss of weight with increase of temperature despite the second step begins circa at 260 °C for both kind of membranes. Consequently, a residue of 65 and 27 wt.% at 290 and 450 °C, respectively, are obtained for pristine polymers blend against 73 and 36 wt.% at the same temperatures when the amount of 1.0 wt.% GO filler is added to the polymer matrix. GO loading was increased up to 5.0 wt.% and then the GO/CS:PVA blended membrane was prepared with no significant difference or improvement compared to the GO/CS:PVA blended membrane with a loading of 1.0 wt.%. Such improvements in thermal stability are mainly attributed to the effect of physical barrier of GO nanosheets that leads to a decomposition delay of membrane with temperature. In this regard, Bao *et al.* [58] performed a comparative study between the influence of using pristine G and GO within a PVA polymeric matrix demonstrating that the hydrogen bonds between PVA polymer and the oxygenated functionalized groups present in the G nanosheets were not only responsible for the adequate dispersion and exfoliation of this carbon nanofiller in the polymer matrix, but they also play a role as far the thermal stability is concerned. Thus, GO act as a physical barrier increasing the transition temperature, and consequently improving the thermal stability of the composite membrane [59].

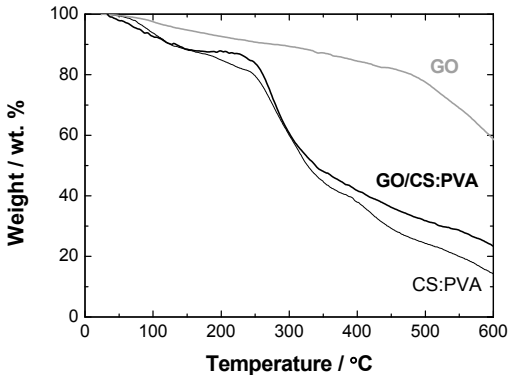

Figure 6. Comparative of thermal decomposition of the CS:PVA, and GO/CS:PVA membranes under nitrogen atmosphere. Thermal decomposition of GO is also shown for comparison.

Water uptake (W_U) of the anion-exchange membranes are correlated with the crystallinity or the crosslinking degree of the membrane matrix, as well as the nature and concentration of the fixed ion exchange groups, the counter ions and membrane homogeneity and the composition of the solution [57]. Particularly, the concentration of the solution exhibits a significant effect on the water sorption due to osmotic effects, which is related to chemical potential difference of the water in the membrane and in the solution [57]. W_U value is measured by the weight difference between the wet and dried OH^- form of the membrane. Hence, W_U of GO/CS:PVA calculated after removing the surface water is 138.40 wt.%, as shown in Table 2, which is similar to that obtained for the unfilled CS:PVA membrane. An increment of up to 5 wt.% of GO content does not lead to a decrease of W_U value (140.5 wt.% for 5 wt.% of GO into the polymer matrix), probably related to no significant

improvement in the degree of crosslinking at high GO loadings. However, when the temperature step was applied to the membrane preparation method for a GO loading of 1.0 wt.% with respect to the polymer matrix, W_U value is 127.6 wt.%, presumably as a consequence of a major lattice of matrix that acts as barrier for water sorption phenomenon. Moreover, the water content (WC) is 19.0 wt.% for the 1.0 wt.% GO/CS:PVA membrane, whereas the CS:PVA membrane showed a WC of 23.11 wt.%, showing no significant differences.

Table 2. Thickness, water uptake, water content, ion exchange capacity, hydroxide conductivity, and permeability of n-propanol through GO/CS:PVA membrane compared to CS:PVA pristine membrane prepared in this study. Membranes PCG 0.1, PCsG 0.1 and FAA are also used for comparison.

Membranes	Thickness (μm)	WC (wt.%)	W_U (%)	IEC (meq· g^{-1})	Specific Conductivity, σ (mS· cm^{-1})	Propanol Permeability, P (10^{-7}· cm^2· s^{-1})
CS:PVA	156 ± 0.001	23.11 ± 4	139.5 [6]	0.253 ± 0.050 [6]	0.15–0.29 [6]	1.76 [6]
GO/CS:PVA	105 ± 0.001	19.00 ± 7.1	138.4	0.379 ± 0.037	0.19	2.43
PCG 0.1 [40]			106.9		42	17.83
PCsG 0.1 [40]			132.3		47.6	17.29
FAA [6]	130 ± 0.001	33.83	16.19	0.318 ± 0.018	2.92	2.34

Other main requirements for anion-exchange membranes are both high permselectivity of counter ions and low electrical resistivity. Membrane performance depends on the adhesion and dispersion of the GO nanofillers in the polymer matrix, which can remarkably determine the mechanical and transport properties of the membrane. Therefore, a feasible, high concentration of fixed ion exchange groups in the polymer backbone chain allows for higher ion exchange capacity (IEC) values, which are related to the capacity of mobility or migration rate of ions within the membrane [60]. Table 2 collects the IEC values for the pristine CS:PVA membrane and hybrid GO/CS:PVA membranes, which increases from 0.253 to 0.379 mmol· g^{-1} upon incorporation of 1.0 wt.% GO into the polymer matrix. However, when temperature was applied for the dispersion of 1.0 wt.% GO in the polymer mixture upon GO-based membrane preparation, the IEC value of GO/CS:PVA membrane decreased to 0.231 mmol· g^{-1}, below the IEC of the unfilled CS:PVA membrane. This fact suggests that temperature has an effect on the membrane framework arrangement, which is in accordance with what was described above for the W_U. Thus, a decrease of the mobility or ion migration is expected because of the obstruction of the free sites necessary for mobility of ions [43].

2.3. Hydroxide Conductivity

The IEC is related to the ion conductivity because of the fixed ion exchange sites in the membrane. However, this relationship is not always linear in semi-crystalline polymers such as those under study. The degree of crystallinity can also contribute to the ionic conductivity of the membranes. The incorporation of nanocarbon fillers creates interconnected channels that favor the ion mobility, and their adequate dispersion in the polymer matrix contributes to facilitate charges and ion transfer in the membrane, which turn higher and effective OH^- conductivity. Nevertheless, the OH^- conductivity of GO/CS:PVA membrane measured by EIS was 0.19 mS· cm^{-1} after membrane activation in 1.0 M NaOH and posterior membrane stabilization in distilled water for 24 h. Clearly, the incorporation of GO sheets seems not to have a significant effect on the ionic conductivity of the membrane and this result can be correlated with the loss of membrane crystallinity in the presence of GO fillers, as shown by XRD described above. It is worth noting that the amorphous region is responsible for ion transport. On the other hand, GO nanosheets allows for ion fixed groups that improve the OH^- mobility within the polymer structure as suggested by the IEC values shown in Table 2.

2.4. Alcohol Permeability

The intrinsic membrane properties, among them the degree of crystallinity, affect significantly the alcohol permeability, a feature that must be as low as possible in membrane electrochemical

applications, more especially in DAFCs and similar configurations. In our previous work [6], we reported how effectively the more amorphous the membranes were, the larger crossover of alcohol into the other compartment. GO, sGO or GO modified with silica (fGO) additives seem to offer an important alcohol barrier effect [29,31,61]. Table 2 also displays the coefficient of propanol diffusion (P) of GO/CS:PVA membrane measured at 120 min. Similar *P* values are obtained at times of 30 and 60 min, as 2.82 × 10^{-7} and 3.38 × 10^{-7} $cm^2 \cdot s^{-1}$, respectively. The *P* values obtained for the GO/CS:PVA membrane are an order of magnitude lower than those reported for the methanol permeation through similar anion-exchange membranes [51]. In fact, our GO-based membrane has a permeability value close to the most common commercial anion-exchange polyelectrolyte membrane, FAA (Fumatech), and similar to that of the unmodified CS:PVA membrane, since, according to XRD results, the structure is reinforced and the tortuosity of the channels leads to lower penetration of alcohol molecules. Furthermore, the hydrogen bonds interactions between the hydrophilic polymer matrix and the GO filler offer more affinity to water than alcohol molecules [54]. All these observations agree with those commented for W_U and WC values collected in Table 2. Finally, to check the crossover of OH^- ions, the solution pH of each compartment was measured, without observing any change in the pH values before and after permeability measurements.

2.5. Electrochemical Performance of GO/CS:PVA Membranes

The performance of the GO/CS:PVA membrane as an alkaline anion-exchange membrane was investigated for the electrooxidation of a model alcohol such as propargyl alcohol (PGA), using a PEMER configuration. Even though the low ionic conductivity and high water uptake of the GO/CS:PVA membrane are evident disadvantages for the use of the membrane in electrochemical processes, the low alcohol permeation through the cathode compartment and excellent physical contact with the carbonaceous electrodes (in fact, only a small pressure applied between the bipolar plates without the need of hot press procedure was necessary), accounting to low membrane rigidity, might lead to an electrochemical performance comparable to that of the commercial membrane FAA. Figure 7 depicts the comparative polarization curve in the presence of 0.25 M PGA for FAA and GO/CS:PVA membranes. The behavior of these membranes are quite similar, with low IR drops between the membrane and electrodes, especially, at lower current values where both membranes provide equal cell potential values. The similar behavior of the GO/CS:PVA and FAA membranes could be explained by a higher electric conductivity of the GO/CS:PVA membrane compared to the value obtained from EIS measurements. It is worth noticing that heterogeneous and reinforced membranes can lead to undervalued or lower electrical conductivities by using EIS techniques.

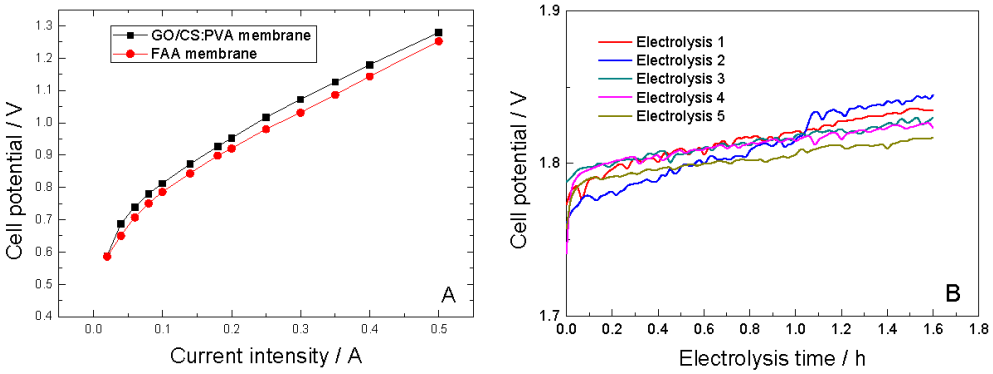

Figure 7. (**A**) Polarization curves of GO/CS:PVA and FAA commercial membranes in 0.25 M propargyl alcohol in 1.0 M NaOH solution. The current intensity range is between 0.02 and 0.50 A, and each current intensity value was kept for 1 min until stabilization of system from which the cell potential is recorded. (**B**) Monitoring of cell potential with electrolysis time.

A number of five consecutive electrochemical oxidations of 0.25 M PGA in 1.0 M NaOH solution were performed upon a Ni-based anode and a gas diffusion cathode electrode for the electro reduction of oxygen. Table 3 summarizes the electrochemical conditions as well as some parameters obtained from the electrooxidation of PGA. Moreover, Table 3 exhibits data related to the electrooxidation of PGA under the same experimental conditions but using the FAA membrane. All electrochemical reactions were carried out at controlled current density of 20 $mA \cdot cm^{-2}$ and cell potentials during the electrooxidation process were constant around a value of 1.8 V (see Figure 7B). This could be an indication of the chemical stability of the membrane in this type of electrochemical processes. The electrochemical performance of the membrane has been evaluated from the PGA conversion and current efficiency values obtained for each of the five consecutive electrooxidative reactions. The PGA conversion values are above 0.5 for a charge passed of 2895 C after two electrolysis, being the main and unique product of reaction (*Z*)-(3-propynoxy) 2-propenoic acid (*Z*-PPA). However, it should be noted that PGA conversion value is almost equal for the five electrolyses conducted. The average current efficiency is 0.23 when using the GO-based membrane, denoting that a secondary reaction such as the oxygen evolution is also taking place together with the electrooxidation of PGA. Table 3 also shows the space-time yield and the electrolytic energy consumption for the electrooxidation of PGA.

The behavior of the commercial membrane displays a lower cell potential of 1.21 V, denoting that IR drops associated to the membrane is lower than GO/CS:PVA membrane. Besides, the PGA conversions and current efficiency obtained using the GO/CS:PVA membrane were similar to those reached for the FAA membrane, though energetic consumption is somewhat higher.

From a practical point of view, the reproducibility of the synthesis of graphene based polymer blend membranes is of great concern for the scaling up and manufacturing of novel alkaline anion-exchange membranes. The nature of the graphene filler should be well identified in terms of the synthesis and together with a fully characterization for extracting important data such as surface area, electric resistivity and surface chemistry. Another point relies on the concentration of graphene and its interaction with the homogeneous polymer matrix. Even though pristine graphene and sulfonated graphene, have been used as additives in blend CS:PVA matrices giving rise to the improvement of ionic conductivity and methanol permeability [51], random dispersion of graphene within the polymeric matrix is still present even at low loading of graphene, providing a lack of reproducibility for the manufacturing of the membrane. However, in our study, homogeneous membranes were obtained with only a small loading of 1.0 wt.% GO in CS:PVA, in part because of the oxidation state of the carbon surface and hence the compatibility of the membrane components. Though the ionic conductivity is only slightly improved by the incorporation of GO into the CS:PVA polymer matrix, the experimental procedure presented here offers a reproducible manufacturing approach correlating the distribution of GO across the membrane with improved thermal stability and comparable permeability to the commercial FAA membrane. Last, but more important point, the repeatability of the hybrid polymeric alkaline anion-exchange membrane is of great matter and determining step for the scale-up and commercialization of novel membranes with a wide number of applications in the industry.

Table 3. Experimental conditions and results obtained from the preparative electrooxidation of PGA using a GO/CS:PVA membrane.

Electrooxidation Conditions	Initial PGA Amount (mole)	Anolyte Flow Rate ($mL \cdot min^{-1}$)	Catholyte Flow Rate ($mL \cdot min^{-1}$)	Current Density ($mA \cdot cm^{-2}$)	Temperature (°C)	Anolyte pH
	0.0075 mole (0.25 M)	12	50	20	25 ± 1 °C	14

	Membrane	Conversion, χ_{PGA}	Current efficiency, φ	Products	Space time yield ($Kg \cdot m^{-3} \cdot day^{-1}$)	Specific electrolytic energy consumption ($kWh \cdot kg^{-1}$)	Average cell potential (V)
Electrooxidation	FAA	0.74	0.31	Z-PPA	14574	3.32	1.21 ± 0.01
	GO/CS:PVA						
	(1)	0.64	0.28	Z-PPA	13163	5.5	1.81 ± 0.01
	(2)	0.52	0.22	Z-PPA	13163	7.0	1.81 ± 0.02
	(3)	0.47	0.20	Z-PPA	9402	7.7	1.81 ± 0.01
	(4)	0.51	0.23	Z-PPA	10813	6.70	1.80 ± 0.2
	(5)	0.45	0.20	Z-PPA	9402	7.66	1.80 ± 0.01

3. Materials and Methods

3.1. Materials and Chemicals

Chitosan (CS, coarse ground flakes and powder, Sigma–Aldrich, Barcelona, Spain) with a molecular weight from 310,000 to >375,000 and 75 % deacetylation degree, based on the viscosity range 800–2000 mPa s, and Poly(vinyl) alcohol (PVA, 99+% hydrolyzed from Sigma-Aldrich) with a molecular weight from 85,000 to 124,000 were used as purchased. Graphene oxide (GO, Graphene laboratories Inc., New York, NY, USA 5 $g \cdot L^{-1}$ dispersed in water, thickness 1 atomic layer at least 60%) was used as received for the synthesis of composite membrane based on chitosan: poly(vinyl) alcohol (CS:PVA) blend matrix. Fumatech Company kindly supplied FAA-3-PEEK-130 membrane (FAA). All other chemicals were purchased from the highest analytical grade available and used as received without any further purification. Doubly distilled water with a resistivity of 18.2 MΩ.cm was used for all solutions preparations.

3.2. Membrane Preparation

GO/CS:PVA MMM were prepared from a blend of 1 wt.% of CS and 4 wt.% of PVA homogenous solutions as described in our previous work [6]. Briefly, CS powder was added to the acidic aqueous solution (2 wt.% of acetic acid) and stirred at room temperature for 24 h. Separately, PVA powder was added to distilled water and refluxed at 85 °C for 2 h. Then, CS and PVA solutions were vacuum filtrated to remove impurities. The blend membrane was prepared at a CS:PVA ratio of 50:50 wt.% by mixing the appropriate amounts of the single polymer solutions and stirring for 24 h. Then, a certain amount of GO aqueous solution was added into polymers mixture and stirring for several days until a brownish homogenous mixture was achieved. Finally, the GO/CS:PVA mixture was degassed in the ultrasound bath and cast on a glass plate using a doctor blade at a 0.15 mm opening, and then solvent was evaporated in a fume hood at least for 2 days.

Ion exchange was performed by immersion of the as-made dried membranes in protonated form into a 1.0 M NaOH bath for 24 h and then thoroughly washed with distilled water to remove the NaOH excess. Finally, the OH^- form of the membranes were stored in distilled water at 5 °C, being ready for further characterization and application. Membrane thickness was measured with an IP-65 digital micrometer (Mitutoyo Corp., Kawasaki, Japan) with a precision of 0.001 mm. The measurement was performed at least 4–5 spots over the membrane surface.

3.3. Physicochemical Characterization of GO Solution and GO/CS:PVA Membrane

Raman spectrum was recorded by using LabRam (HORIBA Jobin-Ivon Inc., Edison, NJ, USA with a confocal microscope (×100 objective) spectrometer with a He/Ne laser at 632.78 nm excitation. GO Raman spectra shows a first order region consisting of two peaks at 1345 and 1606 cm^{-1} corresponding to band D and G, respectively, see Figure 1C. D band refers to the defect character in graphite, whilst G band the stretching vibration in the aromatic layers of the graphite crystalline [50,62]. The lower I_D/I_G ratio, the higher graphitization degree and sp^2 character. The intensity of D band is proportional to amount of defect present in the sample or likely edge defects. In this case, the D band results to be significant, which is because of oxygen functionalized groups of GO nanosheet. I_D/I_G ratio is around 1.12, which agrees with the value of 1.09 reported in the literature [20]. The second order Raman spectra of GO exhibits two main peaks where the components D + G and 2D can be assigned.

Morphology of the GO and GO/CS:PVA membranes were observed by scanning electron microscopy (SEM) using a Zeiss DMS 942 instrument operating at 30 kV. Optical images were obtained by using a MOTIC BA 200 microscope. X-ray photoelectron spectroscopy (XPS) experiments were recorded on a K-Alpha Thermo Scientific spectrometer using AlKα (1486.6 eV) radiation, monochromatized by a twin crystal monochromator and yielding a focused X-ray spot with a diameter of 400 μm, at 3 mA × 12 kV. Deconvolution of the XPS spectra were carried out using a Shirley background. X-ray diffraction (XRD) patterns of GO and membranes were collected on a Philips X

Pert PRO MPD diffractometer operating at 45 kV and 40 mA, equipped with a germanium Johansson monochromator that provides Cu Kα1 radiation (λ = 1.5406 Å), and a PIXcel solid angle detector, at a step of 0.05°. The GO-based membrane was examined at 25 °C by powder X-ray diffraction Bruker D8-Advance with mirror Goebel (non-planar samples) with a generator of x-ray KRISTALLOFLEX K 760-80F (power: 3000 W, voltage: 20–60 KV and current: 5–80 mA) with a tube of RX in the wave length 1.5406–1.54439.

Thermal gravimetric analyses (TGA) were carried out using a DTG 60H Shimadzu instrument (Japan) under nitrogen conditions from 25 to 700 °C at a heating rate of 10 °C· min^{-1} in order to explore the thermal stability of the resulting membrane. The decomposition temperature of both pristine (CS:PVA) and doped composite membrane (GO/CS:PVA) was calculated as the temperature at which 5% weight loss occurs, once the water excess is removed from the membrane. Water content (WC) was calculated from the TGA analysis [6,63].

Water uptake (W_U) of the CS:PVA and GO/CS:PVA membrane was calculated by measuring the change in the weight of the membrane before (dried membrane, W_{dry}) and after hydration (wet membrane, W_{wet}), in OH^- form. The wet weight, W_{wet}, was determined by quickly removing water excess and weighing the membrane in an electronic precision balance. The percentage of water uptake was thus calculated using Equation (1):

$$W_U \, or \, swelling \, (\%) = \frac{W_{wet} - W_{dry}}{W_{dry}} \times 100 \quad (1)$$

Ion exchange capacity (IEC) was measured by back-titration. Pristine and doped composite membranes in dried and weighed forms were immersed in 1.0 M NaOH renewable solution for 24 h at room temperature. This alkaline solution was renewed 3 times. The membrane was thus converted to OH^- form. Then, the membrane was rinsed thoroughly with doubly distilled water and equilibrated for 24 h. In the last step, the membrane was soaked in 0.1 M HCl solution for 24 h and this solution was then titrated by a standardized 0.1 M NaOH solution. IEC values were worked out according to Equation (2):

$$IEC \, (mmol/g) = \frac{\left(V_{NaOH,i} - V_{NaOH,f}\right) \times C_{NaOH}}{W_{dry}} \times 100 \quad (2)$$

where $V_{NaOH,i}$ and $V_{NaOH,f}$ are the volume of 0.1 M NaOH solution consumed during back-titration of HCl solutions without and with membrane, respectively. C_{NaOH} is the concentration of NaOH solution previously standardized by potassium hydrogen phthalate [64].

3.4. Electrochemical Impedance Spectroscopy

The specific ionic conductivity of CS:PVA and GO/CS:PVA membranes were calculated by means of the electrochemical impedance spectroscopy (EIS) as well described in [65,66]. EIS experiments were performed using a microAutolab equipped with a FRA impedance module at open circuit potential (potentiostatic method), and a two electrodes electrochemical cell made of stainless steel-plated electrodes with a projected area of 1.13 cm^2. The amplitude was set at 10 mV and the frequency range was established from 0.1 MHz to 100 Hz. EIS experiments were carried out at controlled temperature of 25 ± 3 °C. CS:PVA and GO/CS:PVA membranes were activated in 1.0 M NaOH solution for 24 h, and then, thoroughly rinsed with ultrapure water and finally stabilized in doubly distilled water for 24 h before EIS measurements. Water was removed out of the membrane surfaces using blotting paper before placing the membrane in the EIS cell for the OH^- conductivity through the plane was due to only the membrane.

3.5. Alcohol Permeability Measurements

Permeability was measured at room temperature using a homemade diffusion cell as described by Garcia-Cruz *et al.* [6]. Briefly, the OH^- form membrane was sandwiched between the two

compartments of a filter-press configuration with a 10 cm^2 projected area. The first compartment (A) was filled with a 0.25 M n-propanol in 1.0 M NaOH solution. The second one (B) was filled with doubly distilled water. Both compartments were filled up at the same time and pressure. The concentration of n-propanol was measured by gas chromatography (GC 2010, Shimadzu, Japan) at different times of 0, 0.5, 1 and 24 h. The permeability coefficients of n-propanol, P ($cm^2 \cdot s^{-1}$) was then calculated from Equation (3)

$$P\left(cm^2/s\right) = \frac{(C_B - C_{B0})}{(t - t_0)} \frac{V_B l}{A C_{A0}} \quad (3)$$

where C_{A0} (ppm) is the initial concentration of *n*-propanol in the compartment *A*, and V_B is the water volume in compartment *B*. *A* (cm^2) and *l* (cm) are the membrane area and thickness, respectively.

3.6. Polarization Curves and Electrolysis into a PEM Electrochemical Reactor

Polarization curves were performed using a PEMER architecture of 25 cm^2 projected area using a current range between 0.02 and 0.5 A as reported in our previous work [6]. GO/CS:PVA membrane was placed between the anode electrode made of Ni nanoparticles supported in a carbon black matrix (Ni/CB) with a Ni loading of 0.1 $mg \cdot cm^{-2}$, and a the cathode made of Pt nanoparticles supported in carbon black matrix (Pt/CB) onto diffusion layer (40/60 Vulcan XC-72R/PTFE, with a carbon loading of 2 $mg \cdot cm^{-2}$). Membrane electrode assembly (MEA) was pressed and assembled between two graphitic column plates whereby both compartments are fed, and that act as anodic and cathodic current intensity collectors. Aqueous anolyte consisted of 1.0 M NaOH solution subjected to a flow rate of 12 $mL \cdot min^{-1}$ by using a peristaltic pump (Ismatel Reglo DIG MS/CA 2–8C). Synthetic air (99.999% from Air Liquid, Spain) was humidified prior to being fed into the cathode with a flow rate of 50 $mL \cdot min^{-1}$ controlled by a digital mass flow rate controller (Smart-trak 2 Sierra Intruments, Inc., Monterey, CA, USA).

Before starting the electrooxidation of PGA, Ni/CB catalytic layer was electrochemically activated. To do this, the anode compartment was fed with a 1.0 M NaOH solution and then a current intensity was set to 0.3 A for 16 min to obtain the electrocatalytic NiOOH species [67]. Current intensity, charge passed and cell potential during the electrosynthesis were controlled and monitored using a Gw instek PSP-2010 power supply as current intensity source. PGA electrooxidation was carried out at room temperature with a controlled current of 0.5 A, *i.e.*, 20 $mA \cdot cm^{-2}$ assuming a projected area of 25 cm^2 and a charge passed of 2895 C. PGA conversion and the formation of the final products were followed by HPLC, according to the experimental procedure described elsewhere [68]. Different performance indicators in an electrolysis were calculated such as current efficiency, energy consumption, and space-time yield [69,70]. The final products were confirmed by ^1H NMR at 400 MHz with a BRUKER AV300 Oxford instrument. For the final workup of the electrooxidative reaction, liquid–liquid extraction of the acidified final anolyte solution was performed in ethyl ether; thereafter, the solvent was dried in anhydrous sodium sulphate and finally concentrated in vacuum at 40 °C.

4. Conclusions

We have achieved the synthesis of a GO/CS:PVA membrane using an easy solution casting method that allows a totally homogeneous membrane matrix. This type of membrane was produced cheaply and with eco-friendly reagents and methods of preparations. Neither temperature nor ultrasonic bath [33,39], nor plasticizers as glycerol [51], nor crosslinkers as glutaraldehyde [54] were used. Despite the fact that the GO/CS:PVA membrane does not exhibit a higher OH^- conductivity than the pristine polymer blend, the membrane does present a good reinforced structure acting as physical barrier to significant reduction of alcohol permeability. Moreover, GO/CS:PVA membrane exhibits higher thermal stability than CS:PVA membrane, enabling its use in electrochemical processes with temperature requirements. Nonetheless, the incorporation of oxygen functionalized G nanosheets does not reduce much the swelling of the membrane. The polarization response curve makes it a good candidate for industrial applications of electroorganic synthesis of products with great interest from

an industrial viewpoint, and direct alcohol fuel cells. Nevertheless, the need of exploring much deeper the effect of GO within the structures of CS and PVA blend polymer would be useful to understand better the effect of this carbon filler within the polymer matrix upon the improvement of electrical conductivity, water uptake, and thermal stability.

Acknowledgments: This work has been funded by the Spanish MINECO through projects CTQ2012-31229 and the "Ramón y Cajal" grant RYC2011-08550 (C.C.C.), at the University of Cantabria, and the PhD fellowship BES-2011-045147 and EEBB-14-09094 mobility grant for L.G.C's research stay at theUniversity of Cantabria.

Author Contributions: Leticia García-Cruz and Clara Casado-Coterillo prepared the polymer composites doped with graphene oxide and then carried out all the physicochemical characterization experiments. Jesus Iniesta carried out the electrochemical measurements. Leticia García-Cruz, Jesus Iniesta, Clara Casado-Coterillo, Vicente Montiel and Ángel Irabien analyzed the data and wrote the manuscript.

Conflicts of Interest: The authors declare no conflict of interest.

References

1. Saleh, F.S.; Easton, E.B. Assessment of the ethanol oxidation activity and durability of Pt catalysts with or without a carbon support using Electrochemical Impedance Spectroscopy. *J. Power Sources* **2014**, *246*, 392–401. [CrossRef]
2. Saez, A.; Garcia-Garcia, V.; Solla-Gullon, J.; Aldaz, A.; Montiel, V. Electrocatalytic hydrogenation of acetophenone using a Polymer Electrolyte Membrane Electrochemical Reactor. *Electrochim. Acta* **2013**, *91*, 69–74.
3. Montiel, V.; Sáez, A.; Exposito, E.; García-García, V.; Aldaz, A. Use of MEA technology in the synthesis of pharmaceutical compounds: The electrosynthesis of *N*-acetyl-L-cysteine. *Electrochem. Commun.* **2010**, *12*, 118–121.
4. Ogumi, Z.; Nishio, K.; Yoshizawa, S. Application of the SPE method to organic electrochemistry—II. Electrochemical hydrogenation of olefinic double bonds. *Electrochim. Acta* **1981**, *26*, 1779–1782. [CrossRef]
5. Ogumi, Z.; Inaba, M.; Ohashi, S.-I.; Uchida, M.; Takehara, Z.-I. Application of the SPE method to organic electrochemistry—VII. The reduction of nitrobenzene on a modified Pt-nafion. *Electrochim. Acta* **1988**, *33*, 365–369. [CrossRef]
6. García-Cruz, L.; Casado-Coterillo, C.; Iniesta, J.; Montiel, V.; Irabien, Á. Chitosan:poly (vinyl) alcohol composite alkaline membrane incorporating organic ionomers and layered silicate materials into a PEM electrochemical reactor. *J. Membr. Sci.* **2016**, *498*, 395–407. [CrossRef]
7. Wang, Y.J.; Qiao, J.; Baker, R.; Zhang, J. Alkaline polymer electrolyte membranes for fuel cell applications. *Chem. Soc. Rev.* **2013**, *42*, 5768–5787. [CrossRef] [PubMed]
8. Kinoshita, K. *Electrochemical Oxygen Technology*; John Wiley and Sons Inc.: Pennington, NJ, USA, 1992.
9. Miyazaki, K.; Abe, T.; Nishio, K.; Nakanishi, H.; Ogumi, Z. Use of layered double hydroxides to improve the triple phase boundary in anion-exchange membrane fuel cells. *J. Power Sources* **2010**, *195*, 6500–6503. [CrossRef]
10. Merle, G.; Wessling, M.; Nijmeijer, K. Anion exchange membranes for alkaline fuel cells: A review. *J. Membr. Sci.* **2011**, *377*, 1–35. [CrossRef]
11. Carmo, M.; Doubek, G.; Sekol, R.C.; Linardi, M.; Taylor, A.D. Development and electrochemical studies of membrane electrode assemblies for polymer electrolyte alkaline fuel cells using FAA membrane and ionomer. *J. Power Sources* **2013**, *230*, 169–175. [CrossRef]
12. Gogotsi, Y.; Presser, V. *Carbon Nanomaterials*; CRC Press: Boca Raton, FL, USA, 2006.
13. Tascón, J.M.D. *Novel Carbon Adsorbents*, 1st ed.; Elsevier: Oxford, UK, 2012.
14. Zhong, Y.L.; Tian, Z.; Simon, G.P.; Li, D. Scalable production of graphene via wet chemistry: Progress and challenges. *Mater. Today* **2015**, *18*, 73–78. [CrossRef]
15. Wang, Z.; Xia, J.; Zhu, L.; Chen, X.; Zhang, F.; Yao, S.; Li, Y.; Xia, Y. A selective voltammetric method for detecting dopamine at quercetin modified electrode incorporating graphene. *Electroanalysis* **2011**, *23*, 2463–2471. [CrossRef]
16. Brownson, D.A.C.; Banks, C.E. Graphene electrochemistry: An overview of potential applications. *Analyst* **2010**, *135*, 2768–2778. [CrossRef] [PubMed]

17. Xue, L.; Lingling, X.; Hongli, L. Electrochemical biosensor based on reduced graphene oxide and Au nanoparticles entrapped in chitosan/silica sol-gel hybrid membranes for determination of dopamine and uric acid. *J. Electroanal. Chem.* **2012**, *682*, 158–163.
18. Chen, S.; Zhu, J.; Wu, X.; Han, Q.; Wang, X. Graphene Oxide-MnO_2 nanocomposites for supercapacitors. *ACS Nano* **2010**, *4*, 2822–2830. [CrossRef] [PubMed]
19. Dai, L.; Chang, D.W.; Baek, J.B.; Lu, W. Carbon nanomaterials for advanced energy conversion and storage. *Small* **2012**, *8*, 1130–1166. [CrossRef] [PubMed]
20. Pandele, A.M.; Ionita, M.; Crica, L.; Dinescu, S.; Costache, M.; Iovu, H. Synthesis, characterization, and *in vitro* studies of graphene oxide/chitosan-polyvinyl alcohol films. *Carbohydr. Polym.* **2014**, *102*, 813–820. [CrossRef] [PubMed]
21. Huang, D.; Wang, W.; Kang, Y.; Wang, A. A chitosan/poly(vinyl alcohol) nanocomposite film reinforced with natural halloysite nanotubes. *Polym. Compos.* **2012**, *33*, 1693–1699. [CrossRef]
22. He, L.; Wang, H.; Xia, G.; Sun, J.; Song, R. Chitosan/graphene oxide nanocomposite films with enhanced interfacial interaction and their electrochemical applications. *Appl. Surf. Sci.* **2014**, *314*, 510–515. [CrossRef]
23. Sheshmani, S.; Amini, R. Preparation and characterization of some graphene based nanocomposite materials. *Carbohydr. Polym.* **2013**, *95*, 348–359. [CrossRef] [PubMed]
24. Saravanan, N.; Rajasekar, R.; Mahalakshmi, S.; Sathishkumar, T.P.; Sasikumar, K.S.K.; Sahoo, S. Graphene and modified graphene-based polymer nanocomposites—A review. *J. Reinf. Plast. Compos.* **2014**, *33*, 1158–1180. [CrossRef]
25. Beydaghi, H.; Javanbakht, M.; Bagheri, A.; Salarizadeh, P.; Ghafarian-Zahmatkesh, H.; Kashefi, S.; Kowsari, E. Novel nanocomposite membranes based on blended sulfonated poly(ether ether ketone)/poly(vinyl alcohol) containing sulfonated graphene oxide/Fe_3O_4 nanosheets for DMFC applications. *RSC Adv.* **2015**, *5*, 74054–74064. [CrossRef]
26. Gahlot, S.; Sharma, P.P.; Kulshrestha, V.; Jha, P.K. SGO/SPES-based highly conducting polymer electrolyte membranes for fuel cell application. *ACS Appl. Mater. Interfaces* **2014**, *6*, 5595–5601. [CrossRef] [PubMed]
27. Lee, S.; Choi, B.G.; Choi, D.; Park, H.S. Nanoindentation of annealed Nafion/sulfonated graphene oxide nanocomposite membranes for the measurement of mechanical properties. *J. Membr. Sci.* **2014**, *451*, 40–45. [CrossRef]
28. Kumar, R.; Mamlouk, M.; Scott, K. Sulfonated polyether ether ketone—Sulfonated graphene oxide composite membranes for polymer electrolyte fuel cells. *RSC Adv.* **2014**, *4*, 617–623. [CrossRef]
29. Chien, H.C.; Tsai, L.D.; Huang, C.P.; Kang, C.Y.; Lin, J.N.; Chang, F.C. Sulfonated graphene oxide/Nafion composite membranes for high-performance direct methanol fuel cells. *Int. J. Hydrogen Energ.* **2013**, *38*, 13792–13801. [CrossRef]
30. Xu, C.X.; Cao, Y.C.; Kumar, R.; Wu, X.; Wang, X.; Scott, K. A polybenzimidazole/sulfonated graphite oxide composite membrane for high temperature polymer electrolyte membrane fuel cells. *J. Mater. Chem.* **2011**, *21*, 11359–11364. [CrossRef]
31. Choi, B.G.; Huh, Y.S.; Park, Y.C.; Jung, D.H.; Hong, W.H.; Park, H. Enhanced transport properties in polymer electrolyte composite membranes with graphene oxide sheets. *Carbon* **2012**, *50*, 5395–5402. [CrossRef]
32. Jiang, Z.; Zhao, X.; Fu, Y.; Manthiram, A. Composite membranes based on sulfonated poly(ether ether ketone) and SDBS-adsorbed graphene oxide for direct methanol fuel cells. *J. Mater. Chem.* **2012**, *22*, 24862–24869. [CrossRef]
33. Liu, Y.H.; Wang, J.T.; Zhang, H.Q.; Ma, C.M.; Liu, J.D.; Cao, S.K.; Zhang, X. Enhancement of proton conductivity of chitosan membrane enabled by sulfonated graphene oxide under both hydrated and anhydrous conditions. *J. Power Sources* **2014**, *269*, 898–911. [CrossRef]
34. Wang, J.; Wang, X.; Xu, C.; Zhang, M.; Shang, X. Preparation of graphene/poly(vinyl alcohol) nanocomposites with enhanced mechanical properties and water resistance. *Polym. Int.* **2011**, *60*, 816–822. [CrossRef]
35. Lim, H.N.; Huang, N.M.; Loo, C.H. Facile preparation of graphene-based chitosan films: Enhanced thermal, mechanical and antibacterial properties. *J. Non-Cryst. Solids* **2012**, *358*, 525–530. [CrossRef]
36. Zhao, X.; Zhang, Q.H.; Chen, D.J.; Lu, P. Enhanced mechanical properties of graphene-based poly(vinyl alcohol) composites. *Macromolecules* **2010**, *43*, 2357–2363. [CrossRef]
37. Salavagione, H.J.; Gomez, M.A.; Martinez, G. Polymeric modification of graphene through esterification of graphite oxide and poly(vinyl alcohol). *Macromolecules* **2009**, *42*, 6331–6334. [CrossRef]

38. Jiang, L.; Shen, X.P.; Wu, J.L.; Shen, K.C. Preparation and characterization of graphene/poly(vinyl alcohol) nanocomposites. *J. Appl. Polym. Sci.* **2010**, *118*, 275–279. [CrossRef]
39. Shao, L.; Chang, X.; Zhang, Y.; Huang, Y.; Yao, Y.; Guo, Z. Graphene oxide cross-linked chitosan nanocomposite membrane. *Appl. Surf. Sci.* **2013**, *280*, 989–992. [CrossRef]
40. Pan, Y.; Wu, T.; Bao, H.; Li, L. Green fabrication of chitosan films reinforced with parallel aligned graphene oxide. *Carbohydr. Polym.* **2011**, *83*, 1908–1915. [CrossRef]
41. Hegab, H.M.; Wimalasiri, Y.; Ginic-Markovic, M.; Zou, L. Improving the fouling resistance of brackish water membranes via surface modification with graphene oxide functionalized chitosan. *Desalination* **2015**, *365*, 99–107. [CrossRef]
42. Huang, K.; Liu, G.P.; Lou, Y.Y.; Dong, Z.Y.; Shen, J.; Jin, W.Q. A graphene oxide membrane with highly selective molecular separation of aqueous organic solution. *Angew. Chem. Int. Ed.* **2014**, *53*, 6929–6932. [CrossRef] [PubMed]
43. Sharma, P.P.; Gahlot, S.; Bhil, B.M.; Gupta, H.; Kulshrestha, V. An environmentally friendly process for the synthesis of an fGO modified anion exchange membrane for electro-membrane applications. *RSC Adv.* **2015**, *5*, 38712–38721. [CrossRef]
44. Ye, Y.S.; Cheng, M.Y.; Xie, X.L.; Rick, J.; Huang, Y.J.; Chang, F.C.; Hwang, B.J. Alkali doped polyvinyl alcohol/graphene electrolyte for direct methanol alkaline fuel cells. *J. Power Sources* **2013**, *239*, 424–432. [CrossRef]
45. Movil, O.; Frank, L.; Staser, J.A. Graphene oxide-polymer nanocomposite anion-exchange membranes. *J. Electrochem. Soc.* **2015**, *162*, F419–F426. [CrossRef]
46. Yun, S.; Im, H.; Heo, Y.; Kim, J. Crosslinked sulfonated poly(vinyl alcohol)/sulfonated multi-walled carbon nanotubes nanocomposite membranes for direct methanol fuel cells. *J. Membr. Sci.* **2011**, *380*, 208–215. [CrossRef]
47. Liu, Y.L.; Su, Y.H.; Chang, C.M.; Suryani; Wang, D.M.; Lai, J.Y. Preparation and applications of Nafion-functionalized multiwalled carbon nanotubes for proton exchange membrane fuel cells. *J. Mater. Chem.* **2010**, *20*, 4409–4416. [CrossRef]
48. Kannan, R.; Kakade, B.A.; Pillai, V.K. Polymer electrolyte fuel cells using nafion-based composite membranes with functionalized carbon nanotubes. *Angew. Chem. Int. Ed.* **2008**, *47*, 2653–2656. [CrossRef] [PubMed]
49. Xiong, X.; Liu, Q.L.; Zhang, Q.G.; Zhu, A.M. Synthesis and characterization of cross-linked quaternized poly(vinyl alcohol)/chitosan composite anion exchange membranes for fuel cells. *J. Power Sources* **2008**, *183*, 447–453. [CrossRef]
50. Maiti, J.; Kakati, N.; Lee, S.H.; Jee, S.H.; Viswanathan, B.; Yoon, Y.S. Where do poly(vinyl alcohol) based membranes stand in relation to Nafion® for direct methanol fuel cell applications? *J. Power Sources* **2012**, *216*, 48–66. [CrossRef]
51. Feng, X.; Wang, X.; Xing, W.; Yu, B.; Song, L.; Hu, Y. Simultaneous reduction and surface functionalization of graphene oxide by chitosan and their synergistic reinforcing effects in PVA films. *Ind. Eng. Chem. Res.* **2013**, *52*, 12906–12914. [CrossRef]
52. Yang, J.M.; Wang, S.A. Preparation of graphene-based poly(vinyl alcohol)/chitosan nanocomposites membrane for alkaline solid electrolytes membrane. *J. Membr. Sci.* **2015**, *477*, 49–57. [CrossRef]
53. Yoo, B.M.; Shin, H.J.; Yoon, H.W.; Park, H.B. Graphene and graphene oxide and their uses in barrier polymers. *J. Appl. Polym. Sci.* **2014**, *131*, 39628–39650. [CrossRef]
54. Yang, J.M.; Chiu, H.C. Preparation and characterization of polyvinyl alcohol/chitosan blended membrane for alkaline direct methanol fuel cells. *J. Membr. Sci.* **2012**, *419–420*, 65–71. [CrossRef]
55. Ryu, H.J.; Mahapatra, S.S.; Yadav, S.K.; Cho, J.W. Synthesis of click-coupled graphene sheet with chitosan: Effective exfoliation and enhanced properties of their nanocomposites. *Eur. Polym. J.* **2013**, *49*, 2627–2634. [CrossRef]
56. Casado-Coterillo, C.; Andres, F.; Tellez, C.; Coronas, J.; Irabien, A. Synthesis and characterization of ETS-10/Chitosan nanocomposite membranes for pervaporation. *Sep. Sci. Technol.* **2014**, *49*, 1903–1909. [CrossRef]
57. Garcia-Cruz, L.; Casado-Coterillo, C.; Iniesta, J.; Montiel, V.; Irabien, Á. Preparation and characterization of novel chitosan-based mixed matrix membranes resistant in alkaline media. *J. Appl. Polym. Sci.* **2015**, *132*, 42240–42249. [CrossRef]

58. Wan, Y.; Creber, K.A.M.; Peppley, B.; Bui, V.T. Chitosan-based solid electrolyte composite membranes I. Preparation and characterization. *J. Membr. Sci.* **2006**, *280*, 666–674. [CrossRef]
59. Bao, C.L.; Guo, Y.Q.; Song, L.; Hu, Y. Poly(vinyl alcohol) nanocomposites based on graphene and graphite oxide: A comparative investigation of property and mechanism. *J. Mater. Chem.* **2011**, *21*, 13942–13950. [CrossRef]
60. Al-Malah, K.; Abu-Jdayil, B. Clay-based heat insulator composites: Thermal and water retention properties. *Appl. Clay Sci.* **2007**, *37*, 90–96. [CrossRef]
61. Choi, Y.-J.; Song, J.-H.; Kang, M.S.; Seo, B.K. Preparation and electrochemical characterizations of anion-permselective membranes with structurally stable ion-exchange sites. *Electrochim. Acta* **2015**, *180*, 71–77. [CrossRef]
62. Kudin, K.N.; Ozbas, B.; Schniepp, H.C.; Prud'homme, R.K.; Aksay, I.A.; Car, R. Raman spectra of graphite oxide and functionalized graphene sheets. *Nano Lett.* **2008**, *8*, 36–41. [CrossRef] [PubMed]
63. Franck-Lacaze, L.; Sistat, P.; Huguet, P. Determination of the pKa of poly (4-vinylpyridine)-based weak anion exchange membranes for the investigation of the side proton leakage. *J. Membr. Sci.* **2009**, *326*, 650–658. [CrossRef]
64. Lin, B.C.; Dong, H.L.; Li, Y.Y.; Si, Z.H.; Gu, F.L.; Yan, F. Alkaline stable C2-substituted imidazolium-based anion-exchange membranes. *Chem. Mater.* **2013**, *25*, 1858–1867. [CrossRef]
65. Yun, S.H.; Shin, S.H.; Lee, J.Y.; Seo, S.J.; Oh, S.H.; Choi, Y.W.; Moon, S.H. Effect of pressure on through-plane proton conductivity of polymer electrolyte membranes. *J. Membr. Sci.* **2012**, *417–418*, 210–216. [CrossRef]
66. Rezaei Niya, S.M.; Hoorfar, M. Study of proton exchange membrane fuel cells using electrochemical impedance spectroscopy technique—A review. *J. Power Sources* **2013**, *240*, 281–293. [CrossRef]
67. Yi, Q.; Zhang, J.; Huang, W.; Liu, X. Electrocatalytic oxidation of cyclohexanol on a nickel oxyhydroxide modified nickel electrode in alkaline solutions. *Catal. Commun.* **2007**, *8*, 1017–1022. [CrossRef]
68. Garcia-Cruz, L.; Saez, A.; Ania, C.O.; Solla-Gullon, J.; Thiemann, T.; Iniesta, J.; Montiel, V. Electrocatalytic activity of Ni-doped nanoporous carbons in the electrooxidation of propargyl alcohol. *Carbon* **2014**, *73*, 291–302. [CrossRef]
69. Sanchez-Sanchez, C.M.; Exposito, E.; Solla-Gullón, J.; Garcia-Garcia, V.; Montiel, V.; Aldaz, A. Calculation of the characteristic performance indicators in an electrochemical process. *J. Chem. Educ.* **2003**, *80*, 529–533. [CrossRef]
70. Walsh, F. *A First Course in Electrochemical Engineering*; Electrochemical Consultancy: Hants, UK, 1993.